

Figure s1. Testosterone increases hematocrit , hemoglobin (A), and serum iron (B) in castrated (Cx) male mice. At baseline and 7 and 14 days after initiation of testosterone injections, 100 uL blood was drawn for hematological analyses (N = 6, *p = 0.003 for comparison between testosterone-treated (T) and control (C) mice on day 14; **p = 0.001 for comparison of day 14 values with baseline values). Serum iron was measured in blood collected on day 14 (mean \pm SEM, N = 6).

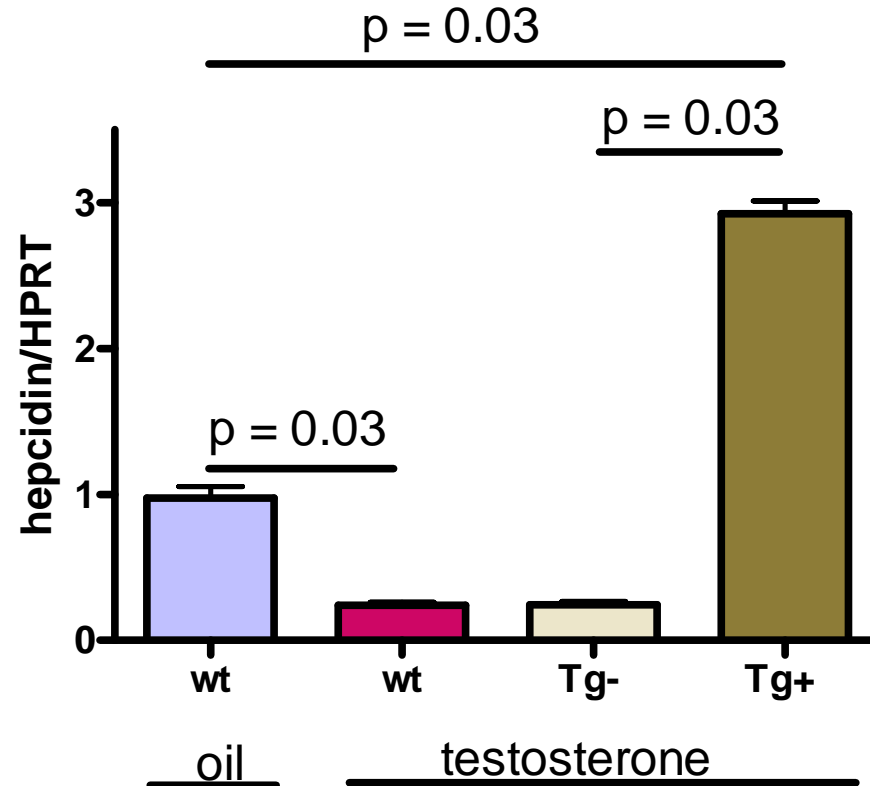


Figure s2. Hepatic hepcidin mRNA expression level in female wild-type (wt) mice and the female mice with silent (Tg-) and constitutively active (Tg+) transgenic hepcidin expression. Testosterone was administered by subcutaneous implant for two weeks (N = 6 for each group). The hepcidin mRNA expression was 3-fold higher in Tg⁺ mice than in Tg⁻ and wild type mice. Testosterone administration was associated with lower hepatic hepcidin expression in wt and Tg⁻ mice but not in Tg⁺ mice. Nearly identical results were found in testosterone-treated castrated male mice (data not shown).

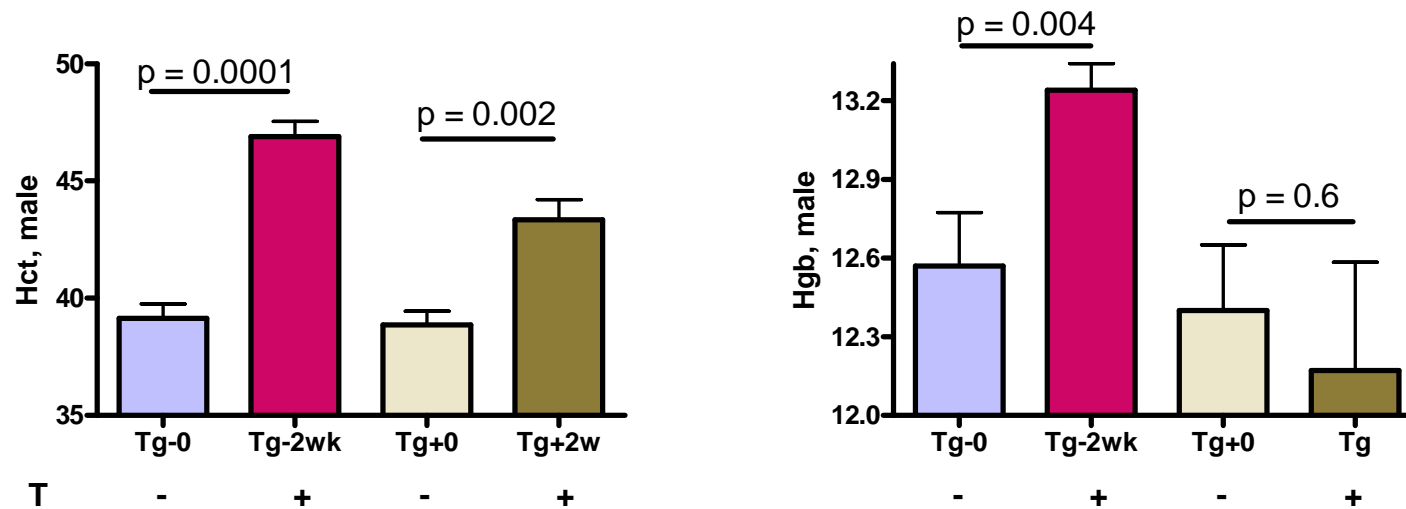
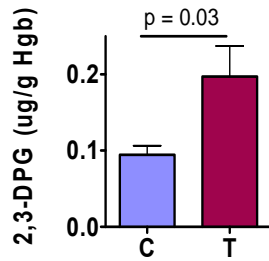
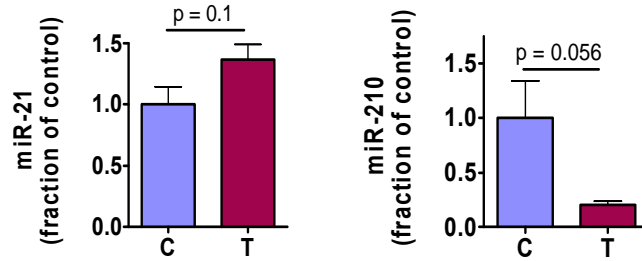


Figure s3. Constitutive over-expression of a hepcidin transgene in Tg+ mice attenuates testosterone-induced increase of hematocrit and completely blocks the rise of hemoglobin (N = 6 for each group). Male mice were castrated, and two weeks later, testosterone implants were inserted subcutaneously. Blood samples were collected at baseline and on day 14. Tg+, transgenic mice that exhibit liver-specific over-expression of a hepcidin transgene (TgN(tTALAP)5Uh;TgN(TRE.Hepc1); Tg-, littermates carrying a silent hepcidin transgene (TgN(TRE.Hepc1 or “Tg-“) that were used as controls.

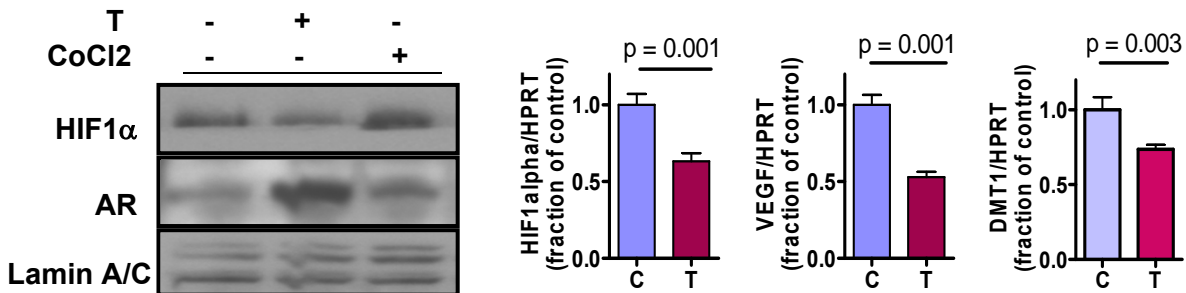
A: Red cell 2,3-DPG



B: Hepatic microRNA



C: Hepatic expression of nuclear HIF1 α and hypoxia-responsive genes



D: Renal hypoxyprobe staining

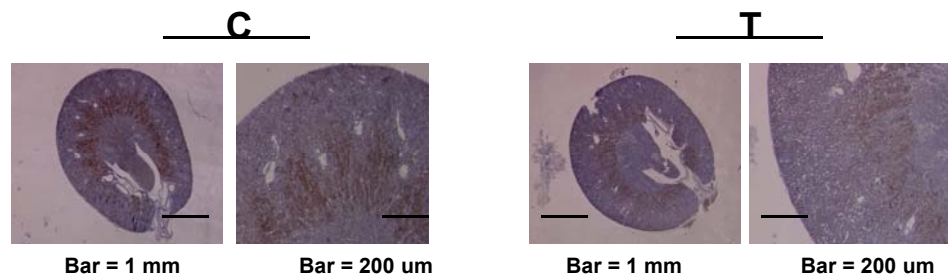


Figure s4. Effects of testosterone administration on hypoxia sensing mechanisms. A. Testosterone treatment for two-weeks for female mice resulted in an increase in red cell 2,3-diphosphoglycerate (2,3-DPG), an effect often found under hypoxic conditions. The results are mean \pm SEM, N=6 for each group. **B.** Hepatic expression of hypoxia-induced microRNA markers, miR-21 and miR-210 (N=4 for each group). Testosterone did not significantly affect miR-21 and exhibited a trend towards miR-210 suppression in the liver of female mice. **C.** Left panel: testosterone treatment for 24 h reduced nuclear HIF1 α in female mice, using CoCl₂ as a positive control. Right panel: testosterone suppressed liver mRNA expression of HIF1 α mRNA as well as their corresponding downstream target genes, VEGF and DMT1. **D.** Hypoxyprobe (pimonidazole) staining in the kidney of mice 24-hours after injection of vehicle or testosterone was lower in testosterone-treated female mice than in vehicle-treated mice, implying testosterone improves tissue oxygenation. Collectively, these results suggest that testosterone suppresses hepcidin expression via a mechanism unrelated to hypoxia sensing.

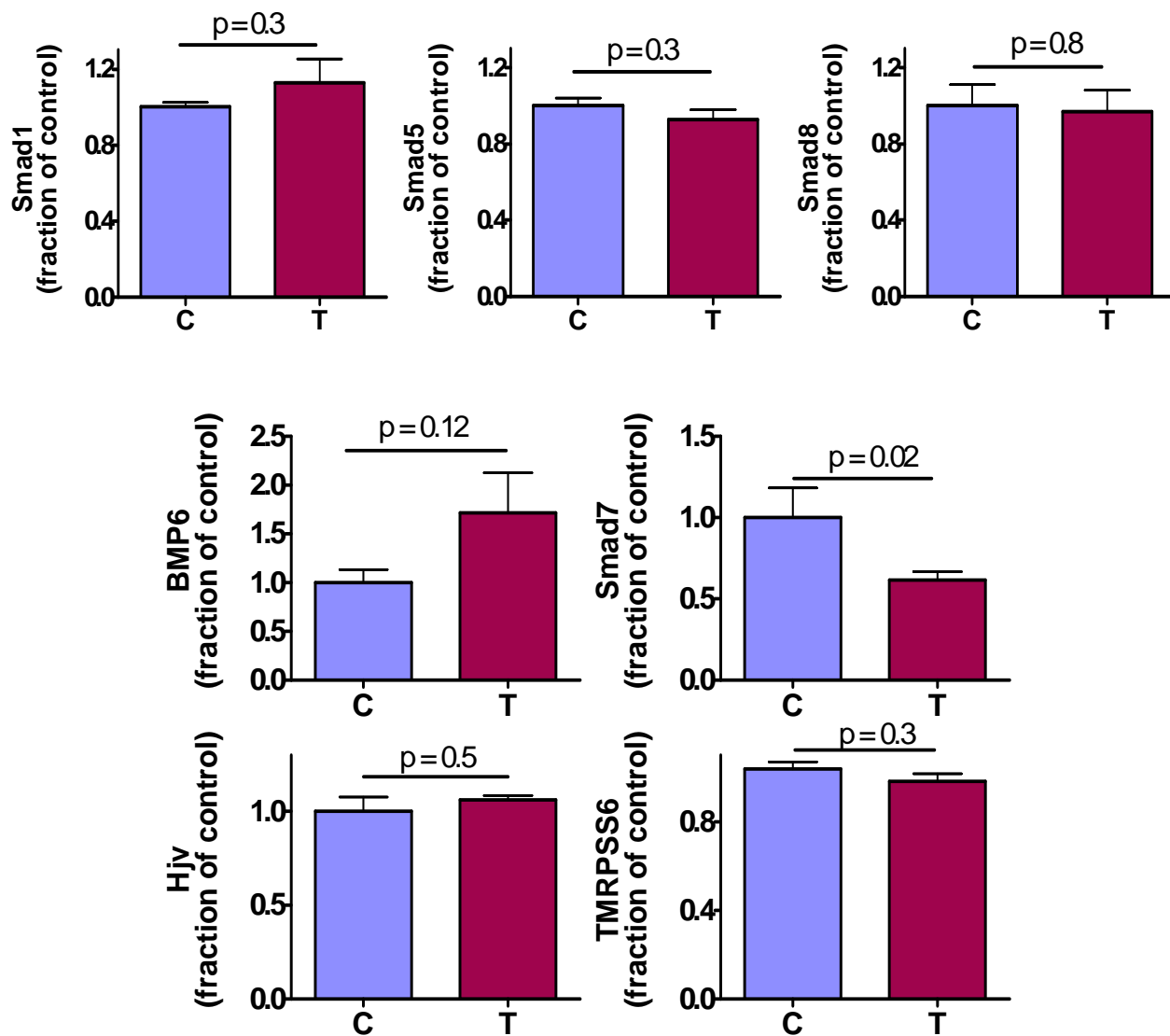


Figure s5. Testosterone does not affect mRNA expression of Smad1, 4, 8, HJV, TMRPSS6, and BMP6, but it significantly reduced the expression of Smad7 in the liver of female mice two days after testosterone injection, a time point when hepcidin expression was down regulated (mean \pm se, N = 6 for each group).

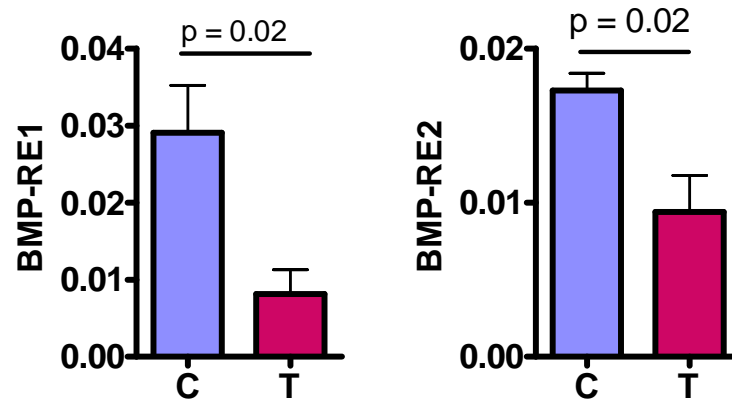


Figure s6. ChIP analysis of liver tissue isolated from mice treated with either vehicle (C) or testosterone (T) four 48 hours. Immunoprecipitation of Smad4 protein-DNA complexes was performed using anti-Smad4 antibody. Real-time PCR was performed using primer sets flanking the BMP-responsive elements of mouse hepcidin promoter as described in the text. Negative and positive control as well as assay specificity were validated as described in the text. Results were normalized to the corresponding inputs (pre-ipsolated chromatin) and shown as means \pm SEM, N = 3 for each group. Testosterone reduced the association between Smad4 and the BMP-RE1 (left panel) and BMP-RE2 (right panel) in the hepcidin promoter.

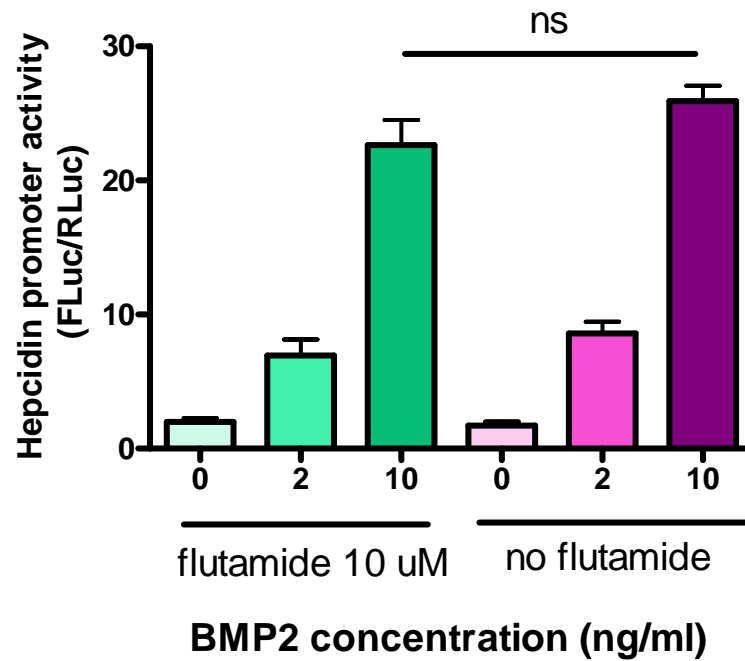


Figure s7. AR antagonist flutamide does not change basal or BMP2-induced hepcidin promoter activity. HepG2 cells were transfected with pGL4 driven by a 3kb wild-type hepcidin promoter and control pRL-CMV Renilla luciferase vector. Cells were incubated in DMEM containing 1% FBS for 12 hours and then supplemented with graded dose of BMP2 for another 12 hours. Results were normalized to Renilla luciferase activity and presented as mean \pm SEM, N = 4 for each condition and analyzed using one-way ANOVA followed by Tukey's test.

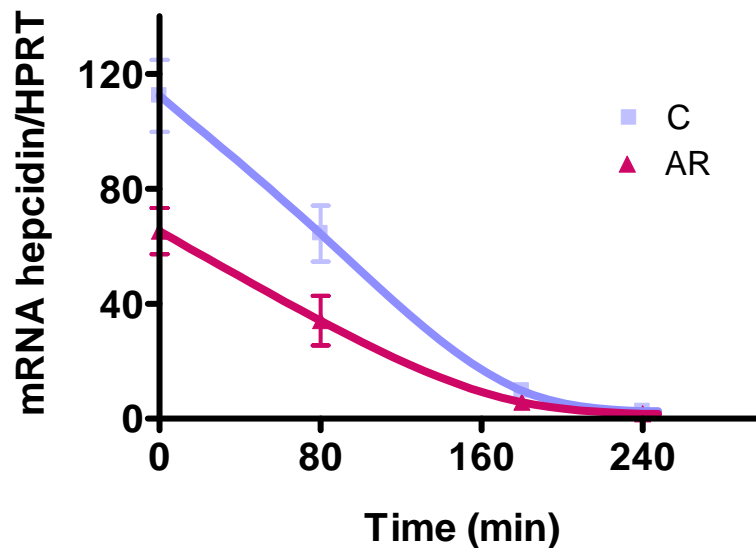


Figure s8. AR/DHT does not affect hepcidin mRNA stability: time-dependent changes in hepcidin mRNA in HepG2 cells expressing vector (C) or ectopic AR after RNA synthesis was blocked by actinomycin D (1 ug/ml). The results are mean \pm SEM, N=4 for each treatment. The slopes are not statistically different. (P=0.57, Wald test of interaction term in a mixed-effects linear regression analysis) in the cells treated with AR/DHT [-1.63 (95% CI: -1.39, -1.88) percent per min] and those treated with medium alone [-1.54 (-1.35, -1.73) percent per min; mean \pm SEM, N=4 for each treatment].

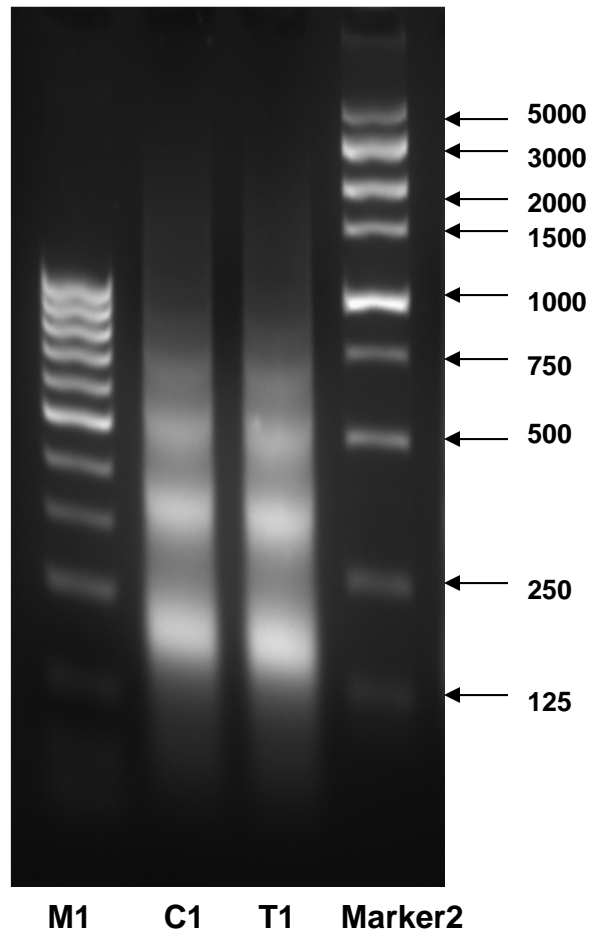


Figure s9. Representative DNA gel pattern after chromatin digestion by micrococcal nuclease at 37C for 30 min (10 min longer than protocol recommended), with frequent flicking. The protein-chromatin complex was then sonicated with 40 pulses using a Fisher Scientific Sonic Dismembrator Model 100, with power setting at 5. Samples were placed on ice between pulses to prevent over heating. Afterwards, DNA was purified by electrophoresis using 1% agarose gel. Distinct bands were visualized near 150, 300, 450, and 600 bp, corresponding to 1 – 4 nucleosomes. On the left is the 100 bp DNA ladder (M1) and on the right is the UMR-150 bp DNA ladder (M2). Results are representative of three independent experiments.